Basic physics of laser propagation in hollow waveguides

J. R. Davies and J. T. Mendonça
Instituto Superior Técnico, GoLP, 1049-001 Lisboa, Portugal
(Received 3 November 1999; revised manuscript received 21 June 2000)

The basic theory of laser propagation in hollow waveguides is considered in the context of laser-plasma physics. The physical model of waves reflecting between the guide walls is used to show that there is a discrete series of modes, and to give the mode dispersion relation and losses in terms of a given reflectivity. The mathematical connection between this model and the solution of Maxwell's equations for lossless propagation in a cylinder is given. Thus the solutions for low loss propagation for any given reflectivity can be obtained, provided it is close to 1. Results are given using Fresnel reflectivity for perfect dielectric and finite conductivity waveguides. The relationship of the breakdown intensity in dielectric waveguides to known breakdown intensities is also derived. The practical implications for the guiding of intense laser pulses and the limitations of the model are discussed. The theory is shown to explain, at least qualitatively, a number of previous experimental results.

PACS number(s): 52.40.Nk, 42.79.Gn, 52.75.−d

I. INTRODUCTION

Free electromagnetic waves of finite extent do not have a unique direction of propagation; they diverge. Thus the intensity of the wave falls and the forward group velocity is less than the speed of light. This is undesirable for a number of laser-plasma applications, in particular the laser wakefield accelerator [1]. To illustrate this, consider a wave propagating perpendicular to the page. The electric and magnetic fields are perpendicular to the direction of propagation, so we can draw the field lines on the page. As $\nabla \cdot \mathbf{B} = 0$ the magnetic field lines cannot have ends, which if they are finite means they must form closed loops. The electric field lines must then be drawn perpendicular to the magnetic field lines, inevitably giving converging (diverging) lines. This means there must be at least two charges on the page (depending on how convoluted the loops are that you drew), which in practice means two or more guides running in the direction of the wave. It is not a free electromagnetic wave. This is the situation in waveguides such as coaxial cables and two wire lines, which are not suitable for guiding intense laser beams. If we cannot have the field running between two or more conductors, we have to bend the field lines out of the page, which then means that propagation is not entirely perpendicular to the page. In a free electromagnetic wave $\nabla \cdot \mathbf{E} = 0$, and both the electric and the magnetic field lines must form closed loops. This follows directly from the wave equation, which does not give propagation without gradients, and vice versa. It also illustrates another important feature of finite electromagnetic waves: you cannot define a unique polarization. In particular, you cannot have a wave which is entirely *s* polarized with respect to a given surface, that is an electric field everywhere parallel to the surface, unless the intensity is uniform over the entire surface. The only way which remains to prevent the wave from continually diverging is to reflect the diverging components between the surfaces of a hollow waveguide. This will maintain the intensity, barring losses, but will still give a forward group velocity less than the speed of light. This has been extensively studied with microwaves, and there are numerous books on the subject, e.g., Elliot [2]. At the other extreme in wavelength, hollow waveguides have been used for guiding x rays; for a recent example and further references, see Ref. [3]. Numerous papers on the guiding of low-intensity laser pulses in hollow waveguides have been published. They have been used, for instance, in achieving ultrashort laser pulses [4], and, at intensities of $\sim 10^{14}$ W cm^{-2}, the generation of gas harmonics by a short pulse laser was studied in glass capillaries [5]. Recently, this subject has become of interest in the field of laser-plasma physics, with the publication of a number of experimental results on the guiding of high intensity, short pulse laser beams in glass capillaries [6–8]. This subject has been studied before in laser-plasma physics, but with long pulse lasers, using gold capillaries [9]. Most of these results were interpreted using a simple geometrical model of rays reflecting between the guide walls, considering either one, average, ray [6,7] or a continuous series [9], and assumng that all rays cross the axis. Dorchies *et al.* [8] based their work on the theoretical results of Marcatili and Schmeltzer [10], which are also referred to in many other papers [4–8]; however, as we will show in Sec. VIII, due to the approximations used there are a number of important errors in these results. Though this subject was extensively studied in the context of microwaves, the emphasis there is on conducting waveguides, which have a significantly different behavior at microwave frequencies than at optical frequencies. The intensity is also not normally considered in this context. To study plasma formation at the guide walls and the breakdown of dielectric waveguides the incident intensity is required. Thus there is a need to reevaluate this theory in the context of laser-plasma physics. In Sec. II we start with a simple physical picture of waves reflecting between the guide walls, showing that there is a discrete series of propagating modes in a hollow waveguide, and obtaining the dispersion relation. This illustrates the geometrical model and its limitations. We then derive the losses in terms of a given reflectivity, the approach used in Refs. [6,7,9]. In Sec. III we consider cylindrical waveguides, giving the solution of Maxwell's equations in a cylinder assuming a homogeneous, isotropic, and linear internal medium.

We then consider two cases for the guide medium: in Sec. IV we assume that there is total reflection from the guide wall, and in Sec. V that the guide is also a homogeneous, isotropic, and linear medium. The first case is of particular interest, as we are interested in low loss propagation, and the experiments we wish to analyze [6–8] inferred high reflectivities. Assuming there is no energy dissipation in the internal medium, it gives a lossless solution, and we analyze this in detail. We show the mathematical connection between it and the physical model of wave reflection between the guide walls, giving the incident intensity at the wall. In Sec. V, for a guide with infinitely thick walls, we show that, with losses to the guide walls, there are only rotationally symmetric modes, and give their dispersion relation. In terms of reflection between the guide walls this can be easily understood, as without rotational symmetry the effective angle of incidence and polarization varies around the wall, and hence the losses vary. Thus nonrotationally symmetric modes distort as they propagate. The dispersion relation for rotationally symmetric modes can, in general, only be solved numerically. In Sec. VI we propose a simple model for low loss propagation, using the lossless solution of Sec. IV to give details of the incident wave at the guide wall and a given reflectivity, as outlined in Sec. II. For nonrotationally symmetric modes we obtain a loss term averaged around the guide wall. The model requires the reflectivity to be a given function of angle of incidence and polarization, and to be close to 1, and the guide radius to be much greater than the wavelength. Thus any theoretical or experimental results for the reflectivity can be used, as deemed appropriate. It represents a generalization of the procedure used in microwave applications [2], where losses to a conducting waveguide are calculated from the surface currents, given by the lossless solution, and the surface impedance of a plane surface. In using the reflectivity in place of the surface impedance, we greatly extend the applicability of the model. As an example, in Sec. VII, we use Fresnel's equations to derive loss terms for ideal dielectric and, in the classical skin effect regime, metal, or plasma waveguides. We show that this approach gives the same results for the rotationally symmetric modes as an approximate solution of the dispersion relation given in Sec. V. For conductors we show that, for the same approximations, we obtain the same results as given for microwaves in Ref. [2]. The issue of dielectric breakdown is considered, and a relation between known breakdown thresholds and that in a dielectric waveguide is given. In Sec. VIII we compare our results with those of Marcatili and Schmeltzer, and point out the errors in their approximations. In Sec. IX we show how the theory can be applied in interpreting experimental results. Finally, Sec. X gives conclusions.

II. BASIC CONSIDERATIONS

The wave vector of waves reflecting between the guide walls can be written as $\mathbf{k}=(k_z;\pm\mathbf{k}_\perp)$, where k_z is the wave number along the waveguide axis, and $\mathbf{k}_\perp$ is the wave vector perpendicular to it. As we saw in Sec. I, there does not exist a solution with $k_\perp=0$. The perpendicular wave number gives an effective perpendicular wavelength of $2\pi/k_\perp$, which must fit the waveguide cross section. Thus only specific values of $k_\perp$ are allowed, giving a discrete set of propagating modes. As a simple illustration, for a parallel plate waveguide there must be a half integer number of wavelengths between the plates, giving $k_\perp=n\pi/L$, where n is an integer mode number and L the separation between the plates. This can easily be extended to a waveguide with rectangular cross section, where $\mathbf{k}_\perp$ has two such components. For a cylindrical waveguide the answer is not so obvious, as there is a continuous range of path lengths possible across a circle, but it is clear that the answer should be similar in form, depending on integer, aziumthal, and radial mode numbers and the reciprocal of the radius. This shows the limitation of the geometrical model (*rays* reflecting between the walls); in reality only certain angles are allowed. Waves with a given value of $\mathbf{k}_\perp$ crossing the guide in opposite directions will interfere to give modes propagating in the axial direction, with wave number k_z, which we will call β, to be consistent with the notation we will adopt below. We must have $k>k_\perp$, so $k_\perp$ represents a cutoff for propagation and we will relabel it k_c. This gives us the mode dispersion relation

$$\beta^2=k^2-k_c^2. \tag{1}$$

From this dispersion relation, or from simple geometrical arguments, we obtain the group and phase velocities

$$v_g=c\sqrt{1-k_c^2/k^2}, \tag{2}$$

$$v_p=\frac{c}{\sqrt{1-k_c^2/k^2}}. \tag{3}$$

These equations are valid in general for lossless propagation, k_c being determined by the guide's cross section. To include losses, the dispersion relation has to be generalized to complex values. Losses will result from energy dissipation in the internal medium and, in the context of this model, from incomplete reflection from the guide wall. The latter can be characterized in terms of a reflectivity R. If this is constant and the number of reflections per unit length, N, is constant, then the intensity of a mode will be given by

$$I(z)=I(0)R^{Nz}. \tag{4}$$

N can be determined from simple geometrical considerations. For our example of a parallel plate waveguide, $N=n\pi/\beta L^2$. In general the reflectivity is a function of angle of incidence, polarization, and intensity. However, if it is a function of intensity this simple model breaks down, as the reflectivity would change at each reflection. This is the approach used to describe the losses in Refs. [6,7,9], where they used just such a two-dimensional model, L in this case being the diameter of the cylinder (capillary). Thus they assumed that all rays cross the axis, but in general there is no reason to assume that this is the case. These simple considerations also show that to achieve the goals of a high group velocity and low losses we require $k\gg k_c$. This requires that the linear dimensions of the waveguide cross section be much greater than the laser wavelength. This is inconsistent with tight focusing, requiring high laser powers to achieve high intensities. To achieve low losses, *s*-polarized waves would also be desirable, as in general the reflectivity is much higher [11]. In three dimensions, this can only be achieved in

a cylindrical waveguide, with a rotationally symmetric intensity, giving a uniform intensity over the surface. This is because the intensity cannot be uniform in both transverse coordinates, as this would imply propagation only in the axial direction. In a rectangular waveguide, one might imagine that an *s*-polarized wave reflecting between only one pair of surfaces would have low losses, as it is not reflecting between the other pair. However, in general, a *p*-polarized wave traveling parallel to a surface does not have zero absorption [2,11], as this maximizes the electric field perpendicular to the surface. This problem is removed if you remove one set of walls, i.e., in two dimensions. This geometry has been used to achieve controlled, monomode guiding of x rays [3], and was also used by Stöckl and Tsakiris [9] to observe plasma formation in a waveguide. We will now concentrate on the case of a cylindical waveguide, of internal radius a. These are the natural choices for guiding a laser beam, and were used in the experiments we wish to examine.

III. WAVES INSIDE A CYLINDER

The general problem is not solved; the interaction of an electromagnetic wave (e.g., a laser) with a surface (e.g., a plasma) is still an active area of research, and a cylindrical surface introduces still further complications. However, for a homogeneous, isotropic, and linear internal medium, described by a complex permittivity and permeability ε and μ, solutions to Maxwell's equations are known. This will be applicable to evacuated waveguides; to waveguides filled with a uniform, very underdense plasma (for which any changes in the plasma conditions will cause a negligible variation in ε and μ); and to most materials at a low enough laser intensity.

The fields are assumed to be of the forms

$$\mathbf{E}=A\hat{\mathbf{E}}(r,\theta)e^{i(\omega t-\gamma z)}, \tag{5}$$

$$\mathbf{B}=\sqrt{\mu\varepsilon}A\hat{\mathbf{B}}(r,\theta)e^{i(\omega t-\gamma z)}, \tag{6}$$

where A is a constant (possibly complex) amplitude, ω is the laser angular frequency, and

$$\gamma=\beta-i\alpha, \tag{7}$$

where β is the axial wave number and α the loss term. Further, assuming a separable solution gives Bessel's equation for the radial dependence of both axial field components. This has either the trivial solution that the axial field is zero, or a solution in terms of Hankel functions [12] (also called Bessel functions of the third kind), giving two independent solutions, one with $B_z=0$ and the other with $E_z=0$. The first gives what are usually referred to as transverse magnetic modes, labeled TM_{nm}, and latter transverse electric modes labeled TE_{nm}. The integers $n(\geqslant 0)$ and m (>0) are radial and azimuthal mode numbers, respectively. The requirement that the solution does not diverge at the origin gives a solution in terms of the Bessel functions J_n and their derivatives J_n'. For transverse magnetic modes $(B_z=0)$,

$$\hat{E}_r=\frac{\gamma}{k_c}J_n'(k_c r)\cos n(\theta+\theta_0), \tag{8}$$

$$\hat{E}_\theta=-\frac{\gamma}{k_c}\frac{n}{k_c r}J_n(k_c r)\sin n(\theta+\theta_0), \tag{9}$$

$$\hat{E}_z=iJ_n(k_c r)\cos n(\theta+\theta_0), \tag{10}$$

$$\hat{\mathbf{B}}=\frac{k}{\gamma}\mathbf{z}\times\hat{\mathbf{E}}, \tag{11}$$

and for transverse electric modes $(E_z=0)$,

$$\hat{E}_r=-\frac{k}{k_c}\frac{n}{k_c r}J_n(k_c r)\sin n(\theta+\theta_0), \tag{12}$$

$$\hat{E}_\theta=-\frac{k}{k_c}J_n'(k_c r)\cos n(\theta+\theta_0), \tag{13}$$

$$\hat{\mathbf{B}}_\perp=\frac{\gamma}{k}\mathbf{z}\times\hat{\mathbf{E}}, \tag{14}$$

$$\hat{B}_z=iJ_n(k_c r)\cos n(\theta+\theta_0), \tag{15}$$

where $\mathbf{B}_\perp$ refers to B_r and B_θ, and k_c is given by

$$\gamma^2=k^2-k_c^2, \tag{16}$$

where $k^2=\omega^2\mu\varepsilon$. This is the generalization to complex values of the dispersion relation [Eq. (1)] given in Sec. II. The imaginary part of k gives the losses from the internal medium and the imaginary part of k_c gives the losses from the guide wall. Apart from the $n=0$ modes, the form given here is not unique; any combination of these forms with any values of A and θ_0 will also be a mode. The only combination which cannot be written in the form given above is the addition of two of the forms given here, one with an imaginary amplitude, the other with a real amplitude and with differing values of θ_0. Of particular interest is the case in which the magnitudes of the amplitudes are equal, and the values of $n\theta_0$ differ by $\pi/2$. The forms given above can be thought of as linearly polarized modes, and this as a circularly polarized mode. We will adopt this notation and concentrate on these two cases. All that remains is to determine k_c from the boundary conditions at $r=a$ that B_r, E_z, and E_θ are continuous. This requires us to make some assumptions about the guide material. The simplest case is that of total reflection, i.e., B_r, E_z, and E_θ are zero at the wall. Though highly idealized, this can be taken as an approximation of the case in which the reflectivity is high, which is of relevance, as we are interested in low loss propagation, and the experiments we wish to examine inferred high reflectivites. We will look at this solution in Sec. IV. About the only other case of interest which is analytically tractable is for a guide material which is also homogeneous, isotropic, and linear. We will look at this for guide walls of infinite thickness in Sec. V.

IV. LOSSLESS SOLUTION

The cutoff wave number can be written

$$k_c = \frac{u}{a}, \tag{17}$$

where for the transverse magnetic modes TM_{nm} u is given by the roots of the equation $J_n(u)=0$, which we write as u_{nm}, and for the transverse electric modes TE_{nm} by the roots of the equation $J_n'(u)=0$, which we write as u'_{nm}. These values are tabulated in various books. The fundamental mode (lowest k_c) is TE_{11} ($u=1.84$); then comes TM_{01} (2.40), TE_{21} (3.05), TM_{11} and TE_{01} (3.84), TE_{31} (4.20), TM_{21} (5.14), TE_{41} (5.32), etc. [2]. For $u \gg 1$, approximate formulas can be found from the large argument form of the Bessel functions, giving

$$u_{nm} \approx (m + n/2 - 1/4)\pi, \tag{18}$$

$$u'_{nm} \approx u_{n-1m}. \tag{19}$$

In the large argument approximation $u'_{nm} = u_{n-1m}$, but this is *only* true for $n=0$. These formulas are only accurate for the higher m values, and the higher n is the higher the value of m has to be.

Assuming that ε and μ are real gives γ real, and thus a lossless solution. In this case the dispersion relation given in Eq. (16) reduces to that given in Sec. II [Eq. (1)]. We will now examine this solution. In two dimensions we can only readily illustrate the transverse fields, i.e., the magnetic field of the transverse magnetic modes and the electric field of the transverse electric modes. For a given n they have the same basic form, the difference being that the magnetic field lines must form closed loops within the guide, whereas the electric field lines can be cut by the guide wall, giving a surface charge. This is the basis of the differing cutoff wave numbers. Apart from this difference, you can change between the modes by swapping the electric and magnetic fields. For $n=0$ the lines are concentric circles. Vector plots of the fields for $n=1$ and 2 are given in Figs. 1 and 2. A simple progression in the field structure is seen, with each loop in the field splitting with increasing n. The intensity is given by

$$I = A_I \left[\left(\frac{n}{k_c r} \right)^2 J_n^2 \sin^2 n(\theta + \theta_0) + J'^2_n \cos^2 n(\theta + \theta_0) \right], \tag{20}$$

where $A_I = \varepsilon |A|^2 \omega \beta / 2k_c^2$, and the argument of the Bessel functions ($k_c r$) is no longer explicitly stated. This can be rewritten in the more convenient form:

$$I = \frac{A_I}{4} [J_{n+1}^2 + J_{n-1}^2 - 2J_{n+1}J_{n-1} \cos 2n(\theta + \theta_0)]. \tag{21}$$

As mentioned in Sec. III, the only combination of these forms which is of interest is a combination with real and imaginary amplitudes, for which the intensities are simply added. The circularly polarized case gives a rotationally symmetric intensity, equivalent to taking the θ-averaged values of the intensities given above. The functional form of the intensity is determined only by the value of n. The value of m and the class of mode determines where the guide wall cuts it off. Figure 3 gives the intensity for the first six $n=0$ modes. Contour plots of the intensity for the first two $n=1$ and 2, linearly polarized modes are given in Figs. 4 and 5. Only the intensity of the $n=1$ modes peaks on axis. The other modes have a ring of $2n$ equal peaks, with zero intensity on axis. The transverse electric modes have a series of m such rings, of succesively lower intensities, and the $n>0$ transverse magnetic modes $m+1$ rings. For transverse magnetic modes the wall is always just beyond a peak in the intensity, and for transverse electric modes is at a minimum.

We have given the intensities in terms of the peak intensity. More often we know the average intensity, that is the power divided by πa^2, and would like to know the corresponding peak intensity of a mode. We write the ratio of the peak intensity to the average intensity as f_a. The peak intensity depends only on n, as all modes of a given n include the

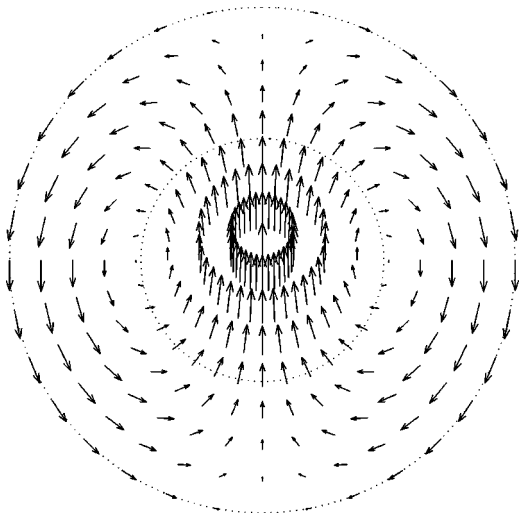

FIG. 1. Vector plot of the transverse $n=1$ fields. The length of the arrow is proportional to the magnitude of the field. Up to the inner dotted circle gives the electric field of the TE_{11} mode, and the outer dotted circle the magnetic field of the TM_{11} mode.

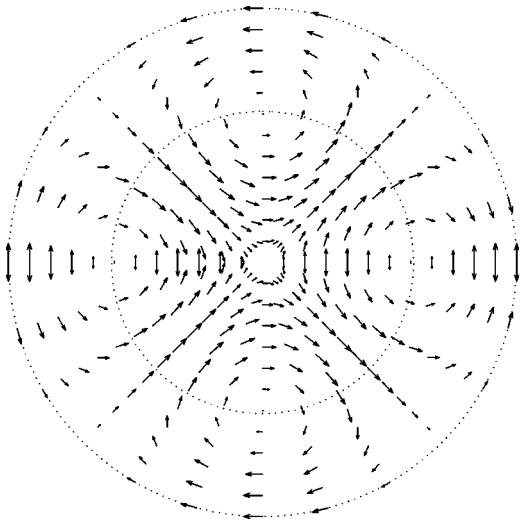

FIG. 2. As in Fig. 1 for $n=2$. The inner dotted circle gives the electric field of the TE_{21} mode, and the outer dotted circle the magnetic field of the TM_{21} mode.

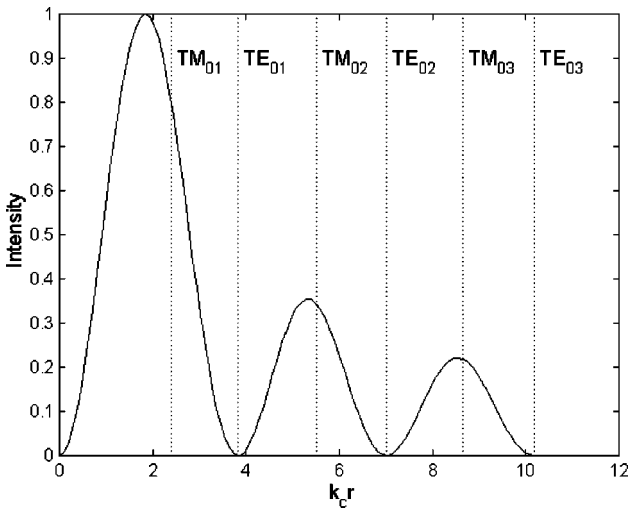

FIG. 3. Mode intensity as a fraction of the peak value for the first six $n=0$ modes.

first, and highest, peak of the intensity. The large argument form of the Bessel functions gives $I_a \propto 1/u$, so we write

$$f_a = a_n u, \tag{22}$$

where a_n is a number which, in the large argument approximation, depends only on n. Evaluating f_a based on the exact expressions [13] for the $n=0$–4, linearly polarized modes, we find that this is accurate to about two significant figures for all except the $m=1$ transverse electric modes, giving

$$a_{0,1,\ldots} \approx 1.0,\ 0.80,\ 0.40,\ 0.36,\ 0.31, \tag{23}$$

except for the TE_{n1} modes, where

$$a_{0,1,\ldots} \approx 1.1,\ 1.1,\ 0.63,\ 0.57,\ 0.54; \tag{24}$$

this gives f_a for $n=0$–4 and any value of m. For the $n>1$ circularly polarized modes the peak intensity is lower than that of a corresponding linearly polarized mode with the

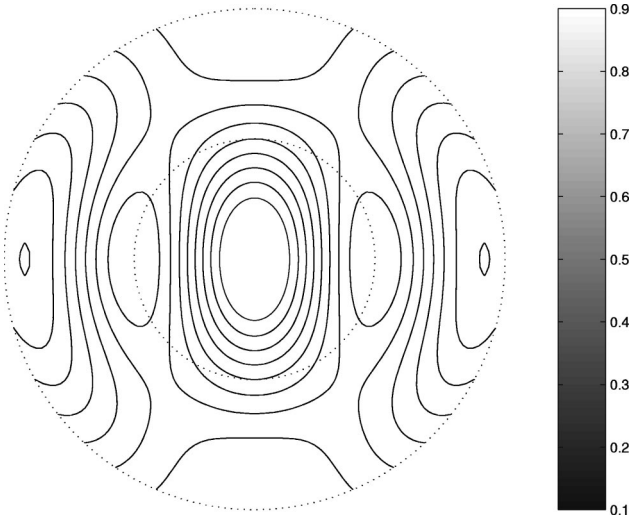

FIG. 4. Mode intensity for the first two $n=1$ modes as a fraction of the peak value. Contours are at intervals of 0.1. The inner dotted circle gives the TE_{11} mode, and the outer dotted circle the TM_{11} mode.

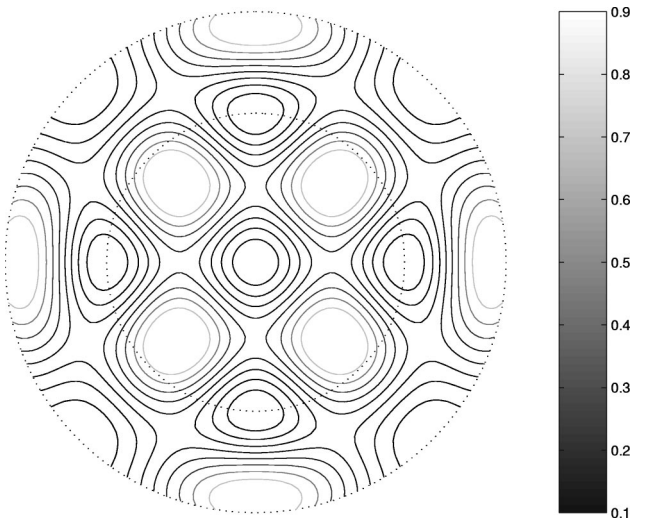

FIG. 5. As in Fig. 4 for $n=2$. The inner dotted circle gives the TE_{21} mode, and the outer dotted circle the TM_{21} mode.

same average intensity. For the $n=2$–4, circularly polarized modes, a_n must be multiplied by 0.677, 0.587, and 0.552 respectively. For $n \gg 1$, this tends to 0.5.

In Sec. II, the fundamental properties of propagation in hollow waveguides were attributed to the fact that propagation is due to wave reflection between the guide walls. This solution is in indeed a superposition of four component waves, traveling in opposite azimuthal and radial directions. The azimuthal components are separated by writing

$$\cos n(\theta+\theta_0) = \frac{1}{2}(e^{in(\theta+\theta_0)} + e^{-in(\theta+\theta_0)}), \tag{25}$$

$$\sin n(\theta+\theta_0) = \frac{1}{2i}(e^{in(\theta+\theta_0)} - e^{-in(\theta+\theta_0)}); \tag{26}$$

thus only the $n>0$ modes have azimuthal components, as they have gradients in the azimuthal direction. The radial components are obtained in an analagous manner, separating the Bessel functions into Hankel functions of the first and second kind, $H_n^{(1)}$ and $H_n^{(2)}$,

$$J_n = \frac{1}{2}(H_n^{(1)} + H_n^{(2)}), \tag{27}$$

$$H_n^{(1),(2)} = J_n \pm i Y_n, \tag{28}$$

where the upper sign refers to $H_n^{(1)}$, and Y_n are either Weber functions, Neuman functions, or Bessel functions of the second kind. They diverge at the origin. With the time dependence $e^{i\omega t}$, $H_n^{(1)}$ represents a radially converging wave and $H_n^{(2)}$ a diverging wave. This is more obvious from the large argument form

$$H_n^{(1),(2)}(x) \approx \sqrt{\frac{2}{\pi x}} e^{\pm i(x-(n+1/2)\pi/2)} + O\left(\frac{1}{x^{3/2}}\right), \tag{29}$$

giving waves with radial wave numbers $\mp k_c$. We are interested in the total incident intensity at the wall, I_w, for which

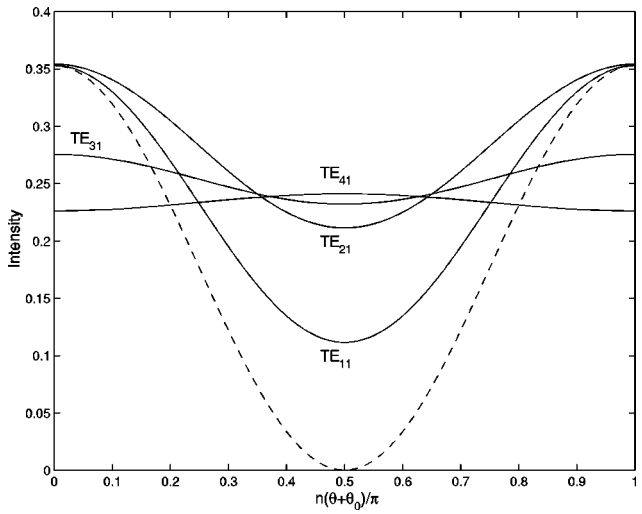

FIG. 6. Axial component of the incident intensity at the wall as a fraction of the peak mode intensity for the first four TE_{n1} modes. The result from the large argument approximation for the TE_{11} mode is given by the dashed line; only its amplitude changes for the other modes.

it is only necessary to consider the $H_n^{(2)}$ component, without separating out the azimuthal components. This gives an intensity

$$\mathbf{I}_w = I_z \hat{\mathbf{z}} + I_r \hat{\mathbf{r}}, \tag{30}$$

where, for the linearly polarized forms,

$$I_z = \frac{I}{4} + \frac{I(Y_n)}{4}, \tag{31}$$

$$I_r = \frac{A_I}{4}\frac{k_c}{\beta}(Y_n' J_n - Y_n J_n')\cos^2 n(\theta + \theta_0), \tag{32}$$

the intensity I and the factor A_I are given by Eqs. (20) and (21), and $I(Y_n)$ signifies these equations in terms of Y_n instead of J_n. For the circularly polarized forms the intensity is again given by taking the θ-averaged values. Using the large argument approximation at the wall ($u \gg 1$) gives

$$I_z \approx A_I \frac{1}{2\pi u}\cos^2 n(\theta + \theta_0), \quad I_r \approx \frac{k_c}{\beta} I_z. \tag{33}$$

For $k_c \ll k$ the axial component dominates, as would be expected for a wave travelling at a small angle to the axis. The large argument approximation is not good for low m values, and is particularly poor for the $n > 0$ transverse electric modes. So we plot the axial intensity at the wall [Eq. (32)] for the $n = 1$–4, linearly polarized, TE_{n1} modes in Fig. 6. For the $n = 0$ and circularly polarized modes the intensity is uniform, though for the circularly polarized modes the energy flux at the wall has the same form: it is just rotating at the laser angular frequency. The main error in the large argument form is overestimating the contrast in intensity; for the TE_{41} modes this has changed to the extent that the peak is at the minimum given by the large argument approximation.

We can see from these results that the mode with the highest group velocity, lowest effective angle of incidence, and lowest number of reflections per unit length will be the TE_{11} mode. However, in general, we would expect the TE_{01} mode to have the lowest losses, as it has only an azimuthal electric field: it is *s* polarized with respect to the guide wall. All modes apart from the $n = 0$ transverse electric modes have a radial electric field at the wall, and for the $n > 0$ modes this varies with θ. This follows from the simple arguments of Sec. II, that when the intensity varies over a surface there is not a unique angle of incidence nor polarization. Thus, for $n > 0$ modes, we would expect absorption and plasma formation at the wall to be asymmetrical, and we could then no longer treat the guide as a cylinder. This indicates that the TE_{01} mode should be preferred for guiding intense laser beams. We will now consider this in more detail for a homogeneous, isotropic, and linear guide medium.

V. WAVES INSIDE THE WALL

If we assume that the guide medium is also homogeneous, isotropic, and linear, then we can solve for the fields in the wall. In this case, we also have the boundary conditions that εE_r (or D_r), B_z/μ, and B_θ/μ (or H_z and H_θ) are continuous. This assumes that there is no additional surface charge (for D) or current (for H) *not* accounted for by the complex permittivity and permeability, i.e., that is not induced by the fields. The solution is basically the same as that given in Sec. III, except that, as the origin is excluded, the Y_n part of the Hankel functions need not cancel. If we assume that the wall is infinitely thick and that there is no wave coming in from infinity, then we obtain a solution in terms of $H_n^{(2)}$, instead of J_n, as inside the cylinder. Applying the boundary conditions shows that there is *no solution with* $n > 0$. The transverse magnetic modes cannot satisfy the continuity of E_z, E_θ, and B_r. The transverse electric modes cannot satisfy the continuity of H_z and H_θ. This means that there is a transverse electric solution with a specified surface current, but no net surface charge. The physical relevance of this solution is not clear, and we will not consider it. This does not mean that there does not exist a nonrotationally symmetric solution of Maxwell's equations, just that there does not exist a solution of the form given by Eqs. (5) and (6). In terms of wave reflection between the guide walls the reason for this is obvious, because, as mentioned in Sec. II, we cannot define a unique angle of incidence nor polarization when the intensity varies over a surface; thus the losses will vary with θ, as we predicted from the lossless results in Sec. IV. This means that the modes would not maintain their shape as they propagated, which is assumed in Eqs. (5) and (6). With the inclusion of losses, the only natural modes in a cylinder are rotationally symmetric. We can obtain a solution for these modes. For the $n = 0$ transverse magnetic modes, k_c is given implicitly by

$$\frac{J_0(k_c a)}{H_0^{(2)}(k_{cg} a)} - \frac{1}{\nu^2}\frac{k_{cg}}{k_c}\frac{J_1(k_c a)}{H_1^{(2)}(k_{cg} a)} = 0, \tag{34}$$

and for the $n = 0$ transverse electric modes by

$$\frac{J_0(k_c a)}{H_0^{(2)}(k_{cg} a)} - \frac{k_{cg}}{k_c}\frac{J_1(k_c a)}{H_1^{(2)}(k_{cg} a)} = 0, \tag{35}$$

assuming that $H_0^{(2)}(k_{cg}a)$ and $H_1^{(2)}(k_{cg}a)$ are not equal to zero. Where $\nu^2=\mu_g\varepsilon_g/\mu\varepsilon$ is the complex refractive index, the subscript g refers to the guide, and k_{cg} is the value of k_c in the guide, given by

$$k_{cg}^2=k_c^2+(\nu^2-1)k^2. \tag{36}$$

In general, Eqs. (34) and (35) have to be solved numerically. The case of total reflection at the wall, considered in Sec. IV, corresponds to the limit that the modulus of the refractive index tends to infinity, provided that the imaginary part is not positive infinite. In this case, the first term of Eq. (34) and the second term of Eq. (35) are dominant, and the Hankel functions tend to zero, giving the results of Sec. IV (note that $J_0'=-J_1$). For the transverse electric modes this only requires that $k_c \ll k_{cg}$, which is true for all situations of interest. For the transverse magnetic modes, however, it requires $\nu k_c/k_{cg} \gg 1$, and we have $k_c \ll k_{cg}$, so the lossless results will only apply for very high refractive indices. Though we cannot find a general, analytic solution, we can find an approximate solution for low loss propagation.

VI. APPROXIMATE LOW LOSS SOLUTION

To obtain an approximate solution for low loss propagation, we start from the lossless solution of Sec. IV, and use the simple loss model, given in Sec. II, $I \propto R^{Nz}$ [Eq. (4)], where R is reflectivity and N the number of reflections per unit length. We assume that the reflectivity is a given function of angle of incidence and polarization, and that it is close to 1, which is more conveniently expressed as $T \ll 1$, where the transmission $T \equiv 1-R$. We obtain the angle of incidence, polarization, and number of reflections per unit length from the lossless solution, by using the incident fields at the wall. By comparing Eq. (4) with Eqs. (5) and (6), we see that in terms of R and N the loss term α is given by

$$\alpha=-\frac{1}{2}N\ln R \approx \frac{1}{2}NT, \tag{37}$$

where we have used the approximation $T \ll 1$ to give α to first order in T. This will give s- and p-polarized loss terms, which we will label α_s and α_p. The losses can be represented in the physically more intuitive form of a loss length L_{loss}, which we define to be the distance for a $1/e$ fall in intensity:

$$L_{loss}=\frac{1}{2\alpha}. \tag{38}$$

In effect, we are using a ray tracing approach, treating the guide wall, point by point, as a plane surface, which requires $a \gg \lambda$. In using the lossless results, we are assuming that the values β and k_c are not significantly changed by the losses; this requires $\alpha^2 \ll k_c^2$, which is also satisfied by the requirement that $a \gg \lambda$. A similar approach is used to obtain the losses for low loss propagation in microwave applications [2]. The starting point is also the lossless solution, which is used to calculate the surface currents instead of the incident fields. The average energy dissipation is then calculated for a given conductivity, assuming that the surface impedence is the same as that for a plane surface, which is analagous to our use of the reflectivity for a plane surface. In addition to the assumptions we make, this also requires the guide to be a homogeneous, isotropic, and linear medium, and that ν^2 is dominated by a large imaginary component. This is a specialized case of the approach given here, which in general is not applicable to laser applications.

Given the reflectivity, all we need to do is to determine φ, N, and the polarization for each of the modes. For the $n=0$ modes this is straightforward, as there are only components in the radial and axial directions, and thus all the rays cross the axis. The angle of incidence φ is given by $\sin\varphi=k_c/k$, the number of reflections per unit length is $N=(k_c/\beta)/2a$, the transverse magnetic modes are p polarized, and the transverse electric modes are s polarized. The $n>0$ modes contain an azimuthal component, and so must include rays which do not cross the axis. To characterize a ray crossing the cylinder at an arbitrary position, we use the angle of incidence ψ of its transverse component to the tangent of the circle, where $0<\psi \leqslant \pi/2$, being equal to $\pi/2$ for a ray that crosses the axis. It is given by the transverse fields at the wall, F_r and F_θ, i.e., the magnetic field for the transverse magnetic modes and the electric field for the transverse electric modes:

$$\sin^2\psi=\frac{F_\theta^2}{F_r^2+F_\theta^2}. \tag{39}$$

The angle of incidence is then given by

$$\sin\varphi=\frac{k_c}{k}\sin\psi, \tag{40}$$

and the number of reflections per unit length by

$$N=\frac{k_c}{\beta}\frac{1}{2a\sin\psi}. \tag{41}$$

The $n>0$ transverse magnetic modes are still p polarized, but the transverse electric modes now have a p as well as an s-polarized component. The parameter $\sin^2\psi$ gives a measure of the degree of s polarization of the transverse electric modes; it is one if the electric field has only an azimuthal component, zero if it has only a radial component, and scales as the intensity ($F_r^2+F_\theta^2$ is proportional to the axial intensity). So we write the loss term for the transverse electric modes as

$$\alpha_{TE}=(\sin^2\psi)\alpha_s+(1-\sin^2\psi)\alpha_p. \tag{42}$$

Thus the problem is solved. However, these parameters depend on phase and θ, which means that the modes consist of rays crossing the cylinder at different positions. Indeed, all that is required of the rays which make up a given mode is that they have the same axial velocity. This clearly illustrates the fact that the $n>0$ modes have components with differing losses, and thus will distort as they propagate. Strictly speaking, however, they are no longer modes. Assuming that the losses are small everywhere, then the distortion over distances less than the loss length will be small, and we can calculate an averaged loss term. There is a further complication for the $n>0$ modes, as at each point there are two rays

incident on the wall, with oppositely directed azimuthal components. In general, the reflectivity of the two rays combined is not expected to be the same as that for each ray individually. For example, at some points two rays with *p*-polarized components interfere to give a purely azimuthal electric field, i.e., an *s*-polarized wave, and at others to give a purely *p*-polarized wave. However, in obtaining an averaged loss term, this problem disappears in the averaging. We take the phase and θ-averaged values of F_r^2 and F_θ^2, to give a root mean square value of $\sin\psi$, weighted according to the intensity, which we will label f_ψ. This gives the same result whether or not you separate out the azimuthal components and for both linearly and circularly polarized modes:

$$\frac{1}{f_\psi^2}=1+\frac{n^2}{u^2}\frac{J_n^2(u)+Y_n^2(u)}{J'^2_n(u)+Y'^2_n(u)}. \tag{43}$$

Using the large argument forms gives $1/f_\psi^2\approx 1+n^2/u^2$, which, strictly speaking, is 1 to the order of the approximation. However, comparison with the exact results shows that this is a reasonable approximation for $u^2\gg n^2$. This is in reasonable agreement for all the $n=1$ modes, but for $n=2$ it already requires $m>3$ to give agreement within 10%. Equations (39)–(42), with f_ψ in place of $\sin\psi$, give an averaged loss term for the $n>0$ modes, and the correct result for the $n=0$ modes. As an example of this approach, we return to the case of a linear, homogeneous, and isotropic guide medium. In this case, for a plane boundary, the reflectivity is given by what are often called the generalized Fresnel equations [11].

VII. LOSSES FROM FRESNEL'S EQUATIONS

Fresnel's equations for *s*- and *p*-polarized transmissions are

$$T_s=\frac{4\nu_r'\sin\varphi}{|\nu'^2|+2\nu_r'\sin\varphi+\sin^2\varphi}, \tag{44}$$

$$T_p=\frac{T_s(\cos^2\varphi+|\nu'^2|)}{|\nu'^2|\sin^2\varphi+2\nu_r'\cos^2\varphi\sin\varphi+\cos^4\varphi}, \tag{45}$$

where $\nu'^2=\nu^2-\cos^2\varphi$, and ν_r' is the real component of ν'. ν being the complex refractive index. The transmission for both *s*- and *p*-polarized waves is zero for $\varphi=0$ (propagation parallel to the surface) and identical for $\varphi=\pi/2$ (normal incidence), as there is no difference between *s* and *p* polarization at normal incidence, between these values the *p*-polarized transmission is higher. The *s*-polarized transmission increases steadily with φ to a maximum at $\varphi=\pi/2$. The *p*-polarized transmission increases more rapidly to a peak, then falls. We require $T\ll 1$, which is always the case for $|\nu^2|$ sufficiently high, for φ sufficiently small, and if ν_r' vanishes, which occurs if ν^2 is dominated by a, negative, real component. We now consider two specific cases of these equations; ideal dielectrics and conductors. We will further assume that $\varepsilon=\varepsilon_0$ and that $\mu=\mu_g=\mu_0$, where the subscript 0 indicates the free space values.

A. Ideal dielectrics

In this case the refractive index is real, with typical values in the range 1.4–2.1 [2]; thus to have $T\ll 1$ we require $k_c\ll k$, where k_c is taken to be the value obtained from the lossless solution. In this approximation the *p*-polarized loss term is

$$a\alpha_p\approx\frac{\nu^2}{\sqrt{\nu^2-1}}\frac{k_c^2}{k^2}, \tag{46}$$

where we have actually used $(\nu^2-1)k_c^2\ll k^2$, rather than simply $k_c\ll k$, and the *s*-polarized loss term is

$$a\alpha_s\approx\frac{1}{\sqrt{\nu^2-1}}\frac{k_c^2}{k^2}. \tag{47}$$

In this approximation, f_ψ in Eqs. (40) and (41) cancels in the expressions for α, so only the $n>0$ transverse electric modes have components with differing losses, the maximum difference being a factor of ν^2. However, for the transverse magnetic modes there is a problem with this approach, because, as we saw in Sec. V, for low values of the refractive index the dispersion relation for the $n=0$ transverse magnetic modes [Eq. (34)] differs significantly from the lossless case. For $(\nu^2-1)k_c^2\ll k^2$ it is the second term of Eq. (34) which dominates, rather than the first term as in the lossless case. Thus we would expect k_c to have approximately the same value as for the transverse electric modes. To check the solution we have obtained here, we will now obtain an approximate low loss solution of Eqs. (34) and (35). Though they only apply to the $n=0$ modes, we take them as a guide to the behavior of the $n>0$ modes. First we simplify the equations. For all situations of interest $k_{cg}a$ is sufficiently high that we can use $H_0^{(2)}/H_1^{(2)}\approx -i$ to a good approximation. Using $k_c^2\ll(\nu^2-1)k^2$ gives

$$f_\nu\frac{k_c}{k}J_0(k_ca)+iJ_1(k_ca)=0, \tag{48}$$

where $f_\nu=\nu^2/\sqrt{\nu^2-1}$ for the transverse magnetic modes and $1/\sqrt{\nu^2-1}$ for the transverse electric modes. We have $f_\nu k_c/k\ll 1$, so the second term is dominant; thus we seek a solution of the form $k_c=k_0+k_1$, where k_0 is given by $J_1(k_0a)=0$, i.e., the value of k_c for the transverse electric modes in the lossless case, and $|k_1|\ll k_0$. Using a Taylor expansion of the Bessel functions about k_0, to first order in k_1, gives

$$f_\nu\frac{k_0+k_1}{k}+iak_1=0. \tag{49}$$

The imaginary part of this equation gives

$$k_{1r}=-f_\nu\frac{k_{1i}}{ka}, \tag{50}$$

where $k_1=k_{1r}+ik_{1i}$. This shows that for $a\gg\lambda$ $(ka\gg 1)$ the change in k_c due to the losses, which are given by k_{1i}, is negligible. Combined with the real part, this gives

$$k_{1i} \approx f_\nu \frac{k_0}{ka}. \tag{51}$$

We want to obtain α, which is given by

$$\alpha = \frac{k_{cr} k_{ci}}{\beta} \approx \frac{k_0}{k} k_{1i} \approx \frac{f_\nu}{a} \frac{k_0^2}{k^2}, \tag{52}$$

which gives the same result as above, only for the transverse magnetic modes k_c is now the same as for the transverse electric modes. The modes are not truly degenerate, as k_1 differs. For the $n>0$ transverse magnetic modes the situation is not clear; the most obvious approach is to simply assume that this result carries over, and we have $u=u'_{nm}$, as for the $n>0$ transverse electric modes. Physically, the difference is that in the lossless case the transverse magnetic field has to form closed loops within the guide, whereas with losses it extends into the guide wall. For good conductors and overdense plasmas the fields in the wall are restricted to a skin depth, so the lossless result remains a good approximation. In this case losses result in energy deposition at the surface. In dielectrics energy loss is due to wave propagation through the guide wall, so the magnetic field extends throughout the guide wall, changing k_c. For the transverse electric modes, the change between dielectrics and conductors is simply that a lower charge density is induced at the wall in dielectrics.

These terms will only apply provided that the intensity is low enough that the dielectric does not break down. This will occur when the intensity in the wall exceeds the breakdown threshold. The required intensity is given by the maximum transmitted intensity. For the breakdown threshold there are numerous theoretical and experimental results, and we will not consider them here. We would like to know the peak intensity in the waveguide at breakdown, so we will consider the ratio between the peak mode intensity and the maximum transmitted intensity, which we will label f_b. Using the large argument approximation and assuming that the intensity at the wall is dominated by the axial component, we obtain the simple form

$$f_b = \frac{f_n}{f_\nu} \frac{a}{\lambda}, \tag{53}$$

where f_n for the linearly polarized modes is given by

$$f_{0,1,\ldots} \approx 3.3,\ 2.5,\ 1.3,\ 1.1,\ 1.0, \tag{54}$$

and for the circularly polarized modes ($n>0$) by

$$f_{1,2,\ldots} \approx 4.9,\ 1.7,\ 1.3,\ 1.1. \tag{55}$$

Comparison with the exact results shows that this is accurate for the $n=0$ modes. For the transverse magnetic modes it is accurate to around 10% for $n=1$ modes, for $n=2$ and 3 modes with $m>1$, and for $n=4$ modes with $m>2$. The TM_{21} values are 1.8 and 1.6 for linearly and circularly polarized modes, respectively. For transverse electric modes the variation in polarization complicates the situation, and the validity depends on the refractive index, agreement being better for lower values. For $\nu=1.5$, it is accurate to around 10% for $n=1-4$ modes with $m>1$. The TE_{11} values are 2.2 and 3.3 and the TE_{21} values are 1.3 and 1.1 for linearly and circularly polarized modes, respectively. These results apply to single modes; higher intensities can be achieved without breakdown by a combination of different modes. This calculation gives a significantly lower peak intensity at breakdown than using the *mode* intensity at the wall [8], which may go to zero even though there is a significant incident intensity, as the incident and reflected waves can cancel one another.

As an example, we will consider $a=20$ μm and $\lambda=1$ μm for a glass waveguide with refractive index $\nu=1.5$. We will consider TM_{01}, TE_{01}, and TE_{11} modes. For the TM_{01} mode we obtain $L_{loss}=0.53$ cm, for the TE_{01} mode $L_{loss}=1.2$ cm, and for the TE_{11} mode $L_{loss}=4$ cm. The $n=0$ results are in excellent agreement with a numerical solution of Eqs. (34) and (35). For typical values of the refractive index the TE_{11} mode is the lowest loss mode in a dielectric, as it has the lowest k_c. For comparison, the characteristic distance for the defocusing of an unguided wave, the Rayleigh length, for a beam with a Gaussian intensity profile, $I \propto e^{-r^2/R^2}$, is $\pi R^2/\lambda$. Taking $R=a/2$ gives a Rayleigh length of 0.031 cm for this case. For the factor f_b we obtain 33 for the TM_{01} mode, 74 for the TE_{01} mode, 54 for the linearly polarized TE_{11} mode, and 110 for the circularly polarized form. Breakdown intensities up to $\sim 10^{14}$ W cm^{-2} have been obtained for glass, depending on the pulse length [14]; thus in this example peak mode intensities up to $\sim 10^{16}$ W cm^{-2} would appear to be the limit. The only way to achieve high intensities in dielectric waveguides is to have $a \gg \lambda$, which requires high laser power; this is their major drawback for most laser-plasma applications. For guiding in dielectric waveguides the circularly polarized TE_{11} mode is preferred, having the highest group velocity, lowest losses, and highest breakdown threshold. It has an intensity profile $I \propto J_0^2 + J_2^2$, which can be well fitted by the typical Gaussian profile with $R=0.77a$. However, as the TM_{11} mode in dielectrics is expected to have virtually the same intensity profile, it will be difficult to excite only this mode.

B. Conductors

In this case

$$\nu^2 = 1 - \frac{\omega_{pg}^2}{\omega^2 + \omega_{col}^2} - i \frac{\omega_{col} \omega_{pg}^2}{\omega(\omega^2 + \omega_{col}^2)}, \tag{56}$$

where ω is the laser angular frequency, ω_{pg} is the guide plasma frequency, and ω_{col} is an effective collision frequency. With the correct choice of parameters, this formula can fit a wide range of metal and plasma results, e.g., the classical and ''anomalous'' skin effects [11]. In fact, most reflectivity results have a dependence on angle of incidence similar to Fresnel's equations [Eqs. (44) and (45)], particularly if you take into account that in most real situations you have a mixture of polarizations; therefore the results can be fitted by choosing an appropriate refractive index. The physical significance of such a fit may, however, be doubtful, but it does mean that the applicability of these results is wider than might be expected. Typically, we have $|\nu^2| \gg 1$, giving

$$a\alpha_s \approx \frac{\nu_r}{|\nu^2|} \frac{k_c^2}{k^2}, \tag{57}$$

where again f_ψ cancels, and therefore the separate components have similar losses. In general, the *p*-polarized term cannot be significantly simplified. However, for the dispersion relation of the $n=0$ transverse magnetic modes [Eq. (34)] to tend to the lossless result, we require $\nu k_c \gg k$, giving

$$a\alpha_p \approx \frac{\nu_r}{|\nu^2|}\frac{1}{f_\psi^2}, \quad \nu k_c \gg k. \tag{58}$$

For $k_c \ll k$, as $\nu k_c \gg k$ must apply to the real and the imaginary parts, this require $\omega_{col} \gg \omega$. For $\nu k_c \ll k$, in which case we expect k_c to be given by the transverse electric result, we obtain

$$\alpha_p \approx |\nu^2| \alpha_s, \nu k_c \ll k. \tag{59}$$

These results can be verified for the $n=0$ modes following the same procedure used in Sec. VII A, though the algebra is more involved. For many cases neither approximation is valid, and a numerical solution will be required for the transverse magnetic modes. These results show us that the *s*-polarized losses will be very low, much lower than in dielectrics, but that the *p*-polarized losses will be significantly higher. This means that the lowest loss mode will, in general, be the TE_{01} mode, and that the $n>0$ modes will rapidly distort, the *p*-polarized component being rapidly lost. Conducting waveguides show what is known as high loss discrimination. Thus the TE_{01} mode is preferred. However, it has a hollow intensity profile (Fig. 3), quite different from the Gaussian profiles normally considered. A similar intensity profile has been generated [15], with the intention of generating a ponderomotive trap, and has a number of possible applications. If the intention is to generate a hollow profile, the expected modification of the intensity profile by propagation in a conducting waveguide could be used for this. Equation (56) shows that lower laser frequencies, which imply longer wavelengths, will give lower losses for a given value of a/λ, due to the higher permittivity. Using a longer wavelength would also make the construction of the waveguides easier. This indicates that longer wavelengths should be preferred. However, shorter wavelengths have the advantage that, for a given laser power and value of a/λ, higher intensities can be achieved.

As an example of Eq. (56) we will consider the classical skin effect regime, principally so that we can make a comparison with results obtained for microwaves, where

$$\omega_{col} = \frac{\omega_{pg}^2 \varepsilon_0}{\sigma}, \tag{60}$$

where σ is the conductivity. This should be valid for incident intensities $I_w \lambda^2 \ll 10^{16}$ W cm^{-2} μm^2 [11]. Conductivities are typically in the range 10^6–$10^8 \Omega^{-1}$ m^{-1} and plasma frequencies, at solid density, are typically in the range 10^{16}–10^{17} s^{-1}, giving collision frequencies from 10^{13} to 10^{17} s^{-1}. The laser angular frequency is $1.88\times10^{15}/\lambda$ s^{-1}, where λ is the laser wavelength in microns. This gives a considerable variation in the values of refractive index. For long wavelengths, such as for microwaves, where $\omega_{col} \gg \omega$, we obtain

$$a\alpha_s \approx \sqrt{\frac{\omega\varepsilon_0}{2\sigma}}\frac{k_c^2}{\beta k} \tag{61}$$

and

$$a\alpha_p \approx \sqrt{\frac{\omega\varepsilon_0}{2\sigma}}\frac{k}{\beta}\frac{1}{f_\psi^2}, \tag{62}$$

where we have not made use of the approximation $\beta \approx k$, so that we can make a direct comparison with the result given by Elliot [2] for the transverse electric modes:

$$a\alpha_{TE} = \sqrt{\frac{\omega\varepsilon_0}{2\sigma}}\left[\frac{k_c^2}{\beta k} + \frac{n^2 k}{\beta(u^2-n^2)}\right]. \tag{63}$$

Using $1/f_\psi^2 \approx 1 + n^2/u^2$, with $u^2 \gg n^2$ and $k_c^2 \ll k^2$ we obtain [Eq. (42)]

$$a\alpha_{TE} \approx \sqrt{\frac{\omega\varepsilon_0}{2\sigma}}\left[\frac{k_c^2}{\beta k} + \frac{n^2 k}{\beta u^2}\right], \tag{64}$$

which for $u^2 \gg n^2$ agrees with Eq. (63). The two results are identical for $n=0$. Though the large argument form is not explicitly used in the derivation of Eq. (63), it is implicit in the assumption that the wall can be treated as a plane surface. There is, however, still a slight inconsistency between these two results. This arises from the assumption used in deriving Eq. (63) that the surface impedance E_θ/H_z was given by the value for a plane surface, $\sqrt{\omega\mu_0/2\sigma}$. Evaluating the surface impedance, assuming $\alpha^2 \ll k_c^2$, shows that this is only the case for $u^2 \gg n^2\beta^2/k_c^2$, in which limit the two results agree. The physical reason for the breakdown of the model is the presence of a *p*-polarized term for $n>0$ [the second terms in the brackets in Eqs. (63) and (64)], which would lead to a distortion of the $n>0$ modes.

To give a specific example we will consider an aluminum waveguide, taking the reflectivity from the experimental results of Milchberg *et al.* [16]. They measured the reflectivity of 400-fs, 0.308-μm, up to 7-mJ, *s*- and *p*-polarized laser pulses, incident at 45° on to an aluminum target, at intensities between 10^{11} and 10^{15} W cm^{-2}. They then fitted the data using Eqs. (56) and (60), the idea being to obtain the conductivity as a function of temperature, which increases with increasing laser intensity. This gave a conductivity which varied by a factor of around 100, decreasing with temperature to a minimum between 40 and 60 eV, then increasing in a Spitzer-like fashion, as expected for a plasma. The plasma frequency did not vary significantly, as aluminum already has three free electrons per atom at room temperature. This shows that the behavior of conducting waveguides can vary considerably with laser conditions, i.e., prepulse, intensity, and pulse duration. As we have already mentioned, if the reflectivity depends *explicitly* on the intensity, rather than there simply being a suitable reflectivity for the laser intensity used, as Milchberg *et al.* assumed, then the simple loss model breaks down. As an example of these results we will consider two extreme cases: (1) room temperature, $\sigma = 3.8\times10^7 \Omega^{-1}$ m^{-1}, corresponding to an incident intensity less than 10^{11} W cm^{-2}, and (2) minimum conductivity $\sigma = 5\times10^5 \Omega^{-1}$ m^{-1}, corresponding to an in-

cident intensity $\sim 10^{14}$–10^{15} W cm^{-2}, both with $\omega_{pg}=2.4\times10^{16}$ s^{-1}. For $\lambda=1$ μm, case (1) gives $\nu=0.454-i12.7$ and case (2) gives $\nu=3.53-i4.10$. For $a=20$ μm we have $\nu k_c \ll k$ in both cases, for all lower order modes; thus Eq. (59) applies. For the TM_{01} mode we obtain $L_{loss}=1.7$ cm for case (1) and 0.22 cm for case (2). Numerical solution of Eq. (34) gives 1.9 and 0.27 cm for cases (1) and (2), respectively, with u being 4.25 and 3.96 respectively, compared to the predicted value of 3.83. For the TE_{01} mode we obtain $L_{loss}=380$ cm for case (1) and 9.1 cm for case (2). A numerical solution of Eq. (35) gives 390 and 9.2 cm for cases (1) and (2), respectively, with u being in excellent agreement with the predicted value. For the TE_{11} mode we obtain $L_{loss}=120$ cm for case (1) and 12 cm for case (2), so it is, marginally, the lowest loss mode for case (2). However, the large difference between the *s*- and *p*-polarized losses would be expected to lead to a significant change in the mode profile over this averaged loss distance; the *p*-polarized loss term is roughly 162 times greater than the *s*-polarized value for case (1), and 29.3 times greater for case (2). For glass we obtained 0.53, 1.2, and 4.0 cm for the TM_{01}, TE_{01}, and TE_{11} modes, respectively. This shows that considerably lower losses can be obtained in conducting waveguides than can be achieved in dielectric waveguides, as well as higher losses in some cases. It also illustrates the high loss discrimination and the large range of different values which can occur, this makes it difficult to make any precise predictions for conducting waveguides.

VIII. COMPARISON WITH THE RESULTS OF MARCATILI AND SCHMELTZER

The work of Marcatili and Schmeltzer [10] has become the standard reference work in the area of laser-plasma physics. As the results given here differ from their results, it is necessary to try and explain these differences. The major differences are in the cutoff wave number k_c (k_i in their notation) and the presence of hybrid modes for $n>0$. In terms of our notation, they give $u=u_{n-1m}$ for *all* modes. This only agrees with our results for the $n=0$ transverse electric modes, and for the $n=0$ transverse magnetic modes when $\nu k_c \ll k$. For $n>0$, it agrees approximately when $u \gg 1$ [Eq. (19)]. For $n>0$, Ref. [10] gave only one class of mode, the electric hybrid modes EH_{nm}, with both axial field components and mixed *s*- and *p*-polarized losses. In this case, we found that there were no modes, as a solution of the form given by Eqs. (5) and (6) cannot satisfy the boundary conditions; however, we took the lossless results as an approximation to the low loss case. Indeed, the fields they give for the hybrid modes cannot satisfy both the requirements for the continuity of the azimuthal and the axial electric fields at the boundary. The value of k_c Ref. [10] gave only satisfies the continuity of the axial component. The origin of the hybrid modes is made clear in the lossless limit, that the modulus of the refractive index tends to infinity, when the fields tend to those of the transverse electric modes. The value of u given in Ref. [10] is thus wrong; it should be the same as we give. This is because the authors of Ref. [10] used the large argument approximation in solving the dispersion relation, for which $u'=u_{n-1m}$. This leads to a significant error for the fundamental mode; their fundamental mode is the EH_{11} mode with $u=2.40$, compared to $u=1.84$ for the TE_{11} mode. Given the importance of this mode in many applications, this is a crucial error. Another error in Ref. [10]'s results, which appears in the lossless limit, is that there are no $n>0$ transverse magnetic modes. We did find that the $n>0$ modes would be distorted by the losses and that, for $\nu k_c \ll k$, the real part of k_c was approximately equal for both classes of mode; thus, approximately, there do exist ''modes'' with both axial field components and combined *s*- and *p*-polarized losses. As, strictly speaking, there are no modes with $n>0$, it is possible to construct a variety of approximate $n>0$ ''modes.'' Our approach has the advantage that it correctly reproduces the known lossless limit of the equations, in which case there do exist $n>0$ modes. However, the hybrid modes Marcatili and Schmeltzer gave are wrong: the fields do not satisfy Maxwell's equations. Only the *internal* fields of their $n=0$ modes satisfy Maxwell's equations to first order in k_c/k, the order of their approximation. Furthermore, the $n=0$ transverse electric modes do not satisfy the requirement for continuity of the azimuthal electric field at the boundary, for the given value of k_c. Obtaining k_c from this condition gives fields which do not satisfy Maxwell's equations. The loss terms given in Ref. [10] are the same as we obtained using Fresnel's equations, for $\nu k_c \ll k$. The loss term for the hybrid modes is what one would obtain for a combination of the transverse magnetic and electric modes with $f_\psi=1$, which also arises from the use of the large argument approximation. Thus we see that the results of Ref. [10] are clearly incorrect, but that for $\nu k_c \ll k$ and $u^2 \gg n^2$, with $a \gg \lambda$, they are in general agreement with the results we obtained using Fresnel's equations. This is to be expected from Ref. [10]'s use of the large argument approximation.

IX. COMPARISON WITH EXPERIMENTAL RESULTS

We will now analyze the experimental results we mentioned in Sec. I [6–9] in the context of this model, in particular those of Jackel *et al.* [6] and Borghesi *et al.* [7]. In all the experiments the laser pulse had a, roughly, Gaussian intensity profile centered on the axis of the cylinder. Thus we expect $n=1$ modes with cutoff wave numbers less than the laser wave number, that is $u<2\pi a/\lambda$, to be excited. In each case this gives a large number of possible modes, as the lowest value of a/λ used was 20. Of these modes, we expect most energy to be in modes whose effective angle of incidence falls within the cone angle of the laser beam. This is normally given in terms of an f number, $f_\#$, which can be related to an effective value of u by

$$u=\frac{ka}{2f_\#}. \tag{65}$$

Thus we expect most energy to be in modes with values of u up to just above this value. In practice, due to the short pulse durations used, there is not a unique value of k which will further increase the spread in the modes. This will lead to pulse dispersion. The main points for comparison are the transmitted intensity profiles [6,7] and the results on breakdown [6,8], for which no real analysis was given. The loss results were adequately described by the model used in these papers of rays bouncing between the walls, because there

were a large number of modes present and they did not use capillaries long enough for the losses to significantly reduce this number. In Refs. [6,7,9] the model was used to infer an average reflectivity, though Jackel *et al.* [6] also stated that using Fresnel's equations gave a good match to the experimental results. In the cases where plasma was formed at the walls [6,7,9] the plasma conditions, and hence the reflectivity, were not known, so a direct comparison was not possible, and the model could only be used to infer the average reflectivity. In this case the model will only be valid if the plasma formed at the walls has a scale length much less than the radius of the waveguide. As Dorchies *et al.* [8] tried to match Marcatili and Schmeltzer's EH_{11} mode, and used the loss term given for that mode, their model is equivalent to the model of Refs. [6,7] of a single, average, ray with the use of Fresnel's equations, as used by Jackel *et al.* [6]. This is because they assumed that there was a single mode and, as we have shown, the loss term given by Marcatili and Schmeltzer is equivalent to using Fresnel's equations for the reflectivity. The value of u they tried to match was 2.40, as $u'_{11}=1.84$ and $u'_{12}=5.33$ we expect most of the energy to be distributed in the TE_{11}, TM_{11}, TE_{12}, and TM_{12} modes. The use of a single ray is only accurate for distances up to roughly the initial, average loss distance, as the differing losses of the modes will lead to a fall in the overall loss term with distance. This was observed by Jackel *et al.* [6] and Stöckl and Tsakiris [9]; the inclusion of a continuous range of rays allowed Stöckl and Tsakiris to reproduce their results. The other experiments did not use sufficiently long capillaries to be able to see this within the experimental errors. Thus the agreement of the results of Dorchies *et al.* with the model of Marcatili and Schmeltzer is not suprising, particularly considering that the lengths of the capillaries they used were comparable to the loss distances they obtained. The fact that the pulse propagated virtually unchanged is also to be expected, due both to the lengths of the capillaries used and the low loss discrimination of dielectric waveguides. As they were operating far from cutoff ($k_c \ll k$), no significant pulse dispersion is expected.

Jackel *et al.* [6] and Borghesi *et al.* [7] gave transmitted intensity profiles at intensities where the capillary wall is ionized. In this case we expect a rapid distortion of the initial intensity profile, which is clearly seen in all their results. The profile given by Borghesi *et al.* for $a/\lambda=20$, which consists of two lobes with a line of low intensity in the middle, though simple in form, does not look like any of the lossless modes. However, it does have the symmetry of $n=1$, just without the central peak in intensity, which, intuitively, one might expect from the loss of the p-polarized part. The profile for $a/\lambda=50$ shows a whole series of peaks, which is expected from the large number of high order modes which could be excited and the lower losses, but again does not have the distinct central peak of the lossless, $n=1$ modes. The profile given by Jackel *et al.*, though it shares the same feature of an intensity minimum on axis, looks just like that of the TE_{21} mode given in Fig. 5, which may well be the same as the TM_{21} mode in this case. Jackel *et al.* gave an f number for the output which gives an effective u, from Eq. (65), of 5.82, as $u'_{21}=3.05$ and $u'_{21}=6.71$, this would be consistent with a strong $m=1$ component. The presence of $n=2$ modes indicates a departure from the expected symmetry, which may be due to imperfections or misalignment of the laser beam or imperfections in the capillaries, such as curvature. Another possibility is that it arises from the ionization of the capillary. For, initially, $n=1$ modes this would be expected to first occur at two opposite points on the wall, which could lead to a change in symmetry from $n=1$ to 2. Given that $n=2$ modes are present, the $m=1$ mode would be expected to rapidly dominate due to its lower losses. In the case of Borghesi *et al.* the capillary was ionized by the laser prepulse, which may have created a slightly asymmetric plasma waveguide (the possible plasma expansion was much less than the radius), which could also, in part, account for the observed distortion of the intensity profile. Thus, though a direct quantitative comparison is not possible, the observed distortion of the intensity profile can be qualitatively understood in the context of our model.

Jackel *et al.* [6] obtained the breakdown energy for internal radii $a/\lambda=50$ and 133. The exact values are not clear, but taking them to be given by the sharp turning points in their Fig. 4 gives 0.02 and 0.5 J, respectively. Everything else being equal, according to our model breakdown the energy scales as a^3. Here we have a change in a^3 of $(133/50)^3\approx 19$ and a change in breakdown energy of $0.5/0.02=25$, in reasonable agreement with the expected scaling. A greater increase is actually expected due to the greater number of modes that could be excited in the larger waveguide. The intensity at breakdown is also of the order predicted by our model; an exact comparison is not possible as we do not know exactly what modes were present. Dorchies *et al.* [8] reported no breakdown for average intensities up to $\sim 3\times 10^{14}(a/\lambda)$ W cm^{-2}. For their 120-fs pulse duration the breakdown intensity taken from Ref. [14] was $I_b \sim 3.3\times 10^{13}$ W cm^{-2}, so this result can be expressed as $\sim 9.5(a/\lambda)I_b$. This, according to our model, requires the energy to be distributed between at least three modes, which we expect to be the case. Significantly higher intensities could not be achieved, as they predicted. Thus we conclude that the model is also consistent with the available results on dielectric breakdown.

X. CONCLUSIONS

Cylindrical waveguides, of whatever type, give a significant improvement over unguided propagation in terms of the distance over which the intensity is maintained, the loss length being considerably greater than the Rayleigh length. This would be of significant benefit in a number of laser-plasma applications, in particular to the laser wakefield accelerator, as the loss length could easily be made comparable to the dephasing length [1] by using a suitably large value of a/λ. However, the reduction in the group velocity [Eq. (3)] must be taken into account, giving a lower maximum energy gain. This effect is also minimized by increasing a/λ, for $a/\lambda \gg (u/2\pi)(\omega/\omega_p)$, where ω_p is the plasma frequency of the plasma inside the waveguide; the reduction in the group velocity from that of a plane wave is negligible. Thus, with the use of waveguides, it would not be necessary to work in a regime of strong self-focusing, and higher group velocities could be achieved, as in general tighter focusing implies lower group velocities. The requirement for high values of a/λ will, however, require more powerful lasers. X-ray la-

sers and harmonic generation are other areas which could benefit from the extended interaction distance which cylindrical waveguides offer. They could also have applications simply as a means of guiding intense laser beams; such a use has been suggested in fast ignition schemes, to guide the ignition pulse into a hohlraum or the capsule itself [7]. For the laser parameters typically used in most of these applications, the guide wall will be ionized. It would also be difficult to obtain a plasma-filled waveguide without ionizing the wall. In this case there is a large difference between the *s*- and *p*-polarized reflectivities, which will lead to a high loss discrimination between the modes and rapid distortion of nonrotationally symmetric field configurations. The lowest loss mode is thus expected to be the TE_{01} mode, which also does not suffer from distortion. It can achieve far lower losses than can be achieved in dielectric waveguides. However, it has a hollow intensity profile (Fig. 3), quite unlike the Gaussian profiles usually considered, which will be distorted, as found in experiments [6,7]. This may find applications in itself. The behavior of the waveguides in this case is also expected to vary considerably with the laser parameters. In some cases such conducting waveguides can give lower losses than dielectric waveguides for all modes. This is the case for sufficiently long wavelengths, which is why dielectric waveguides are not considered for microwave applications. Dielectric waveguides, however, have the advantage that there is a much smaller difference between the *s*- and *p*-polarized reflectivities, so Gaussian profiles will not be so rapidly distorted. For dielectrics the lowest loss mode, indicated by the lossless results, is the TE_{11} mode, which has the lowest cutoff wave number, and hence has the highest group velocity. In its circularly polarized form it can be well fitted by a Gaussian profile with $R=0.77a$, and can achieve the highest peak intensities without breakdown; in glass a peak intensity of $5.5(a/\lambda)$ times the breakdown threshold can be achieved. However, it will start to distort over distances greater than the loss length. With losses, there only exist rotationally symmetric modes. This is not a problem when the losses are very low, as with microwaves in conducting waveguides, but, in general, it will be a problem in high intensity laser applications. Thus the generation and possible applications of the TE_{01} mode merit investigation.

The results given here represent a first step in the basic understanding of laser-capillary experiments. To make the next step will require numerical modeling, e.g., with electromagnetic particle in cell (PIC) codes, as is required in the more straightforward case of plane targets [11].

ACKNOWLEDGMENTS

J.R.D. was supported by the European TMR programme ''Marie Curie Research Fellowships'' under Contract No. ERBFMBICT983502.

[1] For a review on plasma based accelerators, see E. Esarey, P. Sprangle, J. Krall, and A. Tang, IEEE Trans. Plasma Sci. **24**, 252 (1996).

[2] R. S. Elliot, *An Introduction to Guided Waves and Microwave Circuits* (Prentice-Hall, Englewood Cliffs, NJ, 1993).

[3] M. J. Zwanenburg, J. F. Peters, J. H. H. Bongaerts, S. A. de Vries, D. L. Abernathy, and J. F. van der Veen, Phys. Rev. Lett. **82**, 1696 (1999).

[4] M. Nisoli, S. De Silvestri, and O. Svelto, Appl. Phys. Lett. **68**, 2793 (1996).

[5] C. G. Durfee III, A. R. Rundquist, S. Backus, C. Herne, M. M. Murnane, and H. C. Kapteyn, Phys. Rev. Lett. **83**, 2187 (1999).

[6] S. Jackel, R. Burris, J. Grun, A. Ting, C. Manka, K. Evans, and J. Kosakowskii, Opt. Lett. **20**, 1086 (1995).

[7] M. Borghesi, A. J. Mackinnon, R. Gaillard, and O. Willi, Phys. Rev. E **57**, R4899 (1998).

[8] F. Dorchies, J. R. Marqués, B. Cros, G. Matthieussent, C. Courtois, T. Vélikoroussov, P. Audebert, J. P. Geindre, S. Rebibo, G. Harmoniaux, and F. Amiranoff, Phys. Rev. Lett. **82**, 4655 (1999).

[9] C. Stöckl and G. D. Tsakiris, Laser Part. Beams **9**, 725 (1991).

[10] E. A. J. Marcatili and R. A. Schmeltzer, Bell Syst. Tech. J. **43**, 1783 (1964).

[11] For reviews on basic laser-plasma interactions, see E. G. Gamaly, Laser Part. Beams **12**, 185 (1994;); P. Gibbon and E. Förster, Plasma Phys. Controlled Fusion **38**, 769 (1996).

[12] A. Sommerfeld, *Partial Differential Equations in Physics* (Academic Press, New York, 1972), Chap. 4.

[13] All expressions were evaluated using MATLAB Version 5.0 (The MathWorks Inc. 1996).

[14] M. Lenzner, J. Krüger, S. Sartania, Z. Cheng, Ch. Spielmann, G. Mourou, W. Kautek, and F. Krausz, Phys. Rev. Lett. **80**, 4076 (1998).

[15] J. L. Chaloupka, Y. Fisher, T. J. Kessler, and D. D. Meyerhofer, Opt. Lett. **22**, 1021 (1997).

[16] H. M. Milchberg, R. R. Freeman, and S. C. Davey, Phys. Rev. Lett. **61**, 2364 (1988).